Temperature dependence of polar-angle distributions of atoms ejected from ion-bombarded Au{111}

S. W. Rosencrance, N. Winograd, and B. J. Garrison
Department of Chemistry, The Pennsylvania State University, University Park, Pennsylvania 16802

Z. Postawa
Institute of Physics, Jagellonian University, ul. Reymonta 4, PL 30-059 Krakow 16, Poland
(Received 28 September 1995)

Molecular dynamics simulations incorporating the effect of temperature on the crystal lattice reproduce temperature-dependent changes in the ejection yield observed in experimentally obtained angular distributions of species ejected from the Au{111} surface. This effect has been only observed on fcc{111} surfaces and is preferentially active along the [110] direction. The underlying microscopic process responsible for the observed temperature-dependent change in the angular spectra is shown to be related to the number of direct ejection events occurring along close-packed crystallographic directions. Approximately 90% of the observed decrease in the yield along the [110] direction, with increased target temperature, results predominately from surface quenching with some minor contribution from subsurface misalignment of direct ejection sequence chains. The observations for Au{111} are generalized to predict the temperature dependence of the ejection yield for atoms ejected from low index metal single crystals.

I. INTRODUCTION

The observation that the angular distributions of particles ejected from a single crystal target subsequent to energetic ion bombardment are anisotropic was first noted by Wehner in the mid 1950's.[1] As a result of this unexpected phenomenon a significant amount of research has been focused on the elucidation of both fundamental and applied aspects of the events surrounding the interaction of keV ions with solid surfaces.[2] There have been relatively few published investigations, however, detailing the effects of target temperature[3] on the resulting angular distributions of the ejected particles. It is not surprising that there is an absence of information since experiments involving variation of sample temperature are often plagued by dynamic surface conditions with respect to both order and cleanliness in addition to the instrumental difficulties associated with traversing a wide range of target temperatures. Furthermore, the lack of experiments detailing the temperature dependence of the angle resolved ejection yield can be attributed to the thought that this dependence was small or even negligible as suggested by the measurements on the angle integrated ejection yield.[4] As a result temperature effects are not incorporated into the most common analytical theories of sputtering.[4–6]

Despite the relatively small number of temperature-dependent investigations, notable experiments have been performed which suggest that in some cases the angular distributions, both azimuthal and polar, are sensitive to the target temperature.[7,8] Lauderback and co-workers observed that the azimuthal angular distributions of Ni^+ ions ejected from the Ni{111} surface with energies of 10 ± 3 eV and within the polar-angle range of $45°\pm7.5°$ displayed a considerable decrease in anisotropy at increased temperatures.[8] Szymczak and Wittmaack recently investigated the effect of temperature on the polar-angle distributions of particles ejected from Au{111} subsequent to 10 keV Ne^+ ion irradiation.[7] The experimental method used to collect these data consists of collecting all of the Au particles that eject on a glass or graphite plate and analyzing the intensity with Rutherford backscattering spectroscopy. In this study the temperature of the sample was observed to have a significant effect on the ejection yield in the [110] direction[9] of ejection. As evidenced in Fig. 1, the peak heights for the [110] spot decreased by approximately a factor of 3.5 as the target temperature was raised from 15 to 550 K. It was also noted that the change with temperature in ejection yield along the [100] direction[10] is negligible relative to the [110] direction.

As previously detailed, the emission of particles from single crystal metals is dictated by the inherent structure in the near surface region.[11–14,16,17] This concept has been used by Lauderback *et al.* in their computer simulations to explain the observed effect of temperature on their experimental data.[8] Specifically, molecular dynamics calculations which incorporate the thermal vibrations of only the top layer of the crystal were performed. The temperature effect was proposed to be the result of a change in channeling and blocking interactions. A different concept has been presented by Szymczak and Wittmaack who propose that the decrease in yield for the [110] spot at higher temperatures could be caused by a decreased efficiency of long range momentum transfer along close packed crystallographic directions.[7] This depletion was proposed to be related to the misalignment effect of the increased vibrational amplitude on these sequences at increased sample temperatures.

A direct comparison of the observations of Lauderback *et al.* with those of Szymczak and Wittmaack is complicated by several factors. For instance, in the Ni experiment atomic ions were measured while for results in the Au experiment all Au particles were collected. Furthermore, the Ni data were collected at a fixed polar angle and as a function of azimuthal angle while the gold data was presented as a function of polar angle at two azimuths. Nonetheless we believe

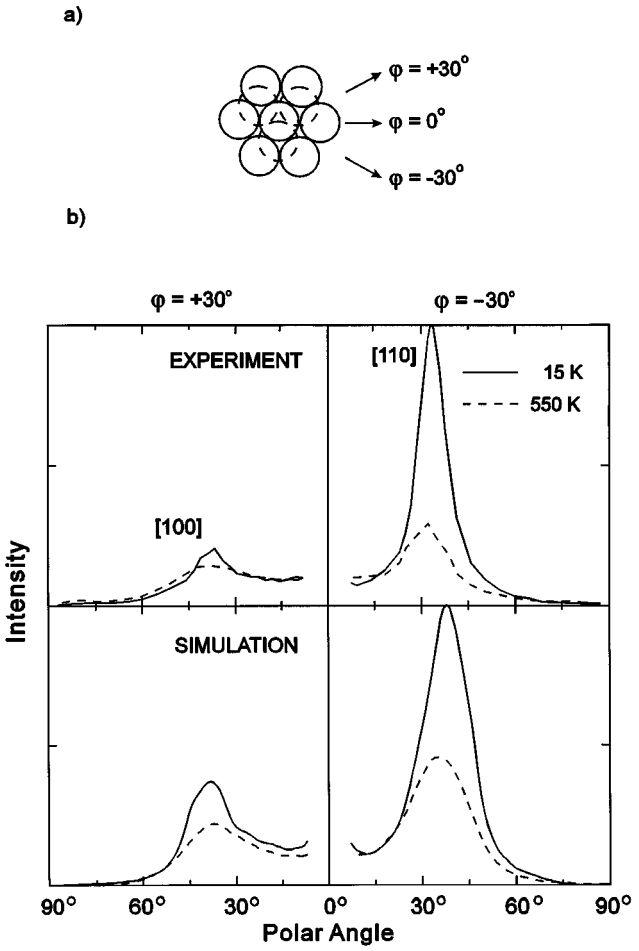

FIG. 1. (a) Azimuthal directions. The broken lines represent the positions of second layer atoms. (b) Energy integrated polar angle spectra for Ne bombarded Au{111} obtained from experiment (top) and simulation (bottom). The calculated spectra include only monomers while the experimental distributions include all ejected particles of Au. The $\varphi=+30°$ azimuth is shown on the left and the $\varphi=-30°$ azimuth is presented on the right ([100] and [110] denotes the crystallographic directions of the peaks or spots as defined in Ref. 7). The angular spectra are obtained from the larger trajectory set and normalized to the number of trajectories. The temperatures are denoted in the legend. The experimental distributions are taken from Ref. 7.

that a common explanation can be used to understand the observed phenomenon for both systems.

Both of the above mentioned studies were performed on {111} surfaces of fcc metals. There have also been both theoretical and experimental investigations of energy resolved angular distributions of atoms ejected from Cu{111} (Ref. 15) and Rh{111} (Ref. 13) at room temperature. These studies show that the intensity of particles ejected along the [110] direction relative to the [100] direction depends on the energy of the ejected particle. For particles that have ~20–50 eV of kinetic energy, the intensities along the [110] and [100] directions are nearly identical. For particles with 5–10 eV of kinetic energy, the intensity along the [110] direction is greater. Although the temperature of the substrate was not varied in these studies any explanation of temperature effect must be consistent with these data.

The purpose of this work is to theoretically explore the temperature related variations of the angular distributions of Au atoms ejected from Au{111} by keV ions as well as to attempt to unify present mechanistic explanations of the temperature effect. To accomplish this goal molecular dynamics (MD) computer simulations using the molecular dynamics/Monte Carlo corrected effective medium (MD/MC-CEM) interaction potential have been performed. These calculations incorporate vibrational displacements in the crystal lattice.[26] The atomic motions subsequent to bombardment have been mechanistically evaluated using a graphical analysis utility.[16,17] The results show that a major ejection mechanism is the direct ejection sequence and detail the mechanistic avenues by which this ejection event is altered as a function of sample temperature.

We find that the effect of temperature on the angular distributions of atoms sputtered from the Au{111} surface is well reproduced using the MD model. The microscopic process responsible for the change in the angular spectra as a function of target temperature is found to be primarily related to the number of direct ejection events occurring along close packed crystallographic directions. Longer direct ejection sequences exhibit a greater temperature effect. This observation suggests that subsurface misalignment is an active mechanism in sputtering. This subsurface misalignment, however, can account for only a small fraction of the observed decrease in ejection yield. Even sequences of unit length (i.e., nearest neighbor collisions) are affected by temperature which clearly implicates the registry of the atoms in the near surface region as the dominant factor in determining the effects of temperature on the resulting observables. These observations are generalized and predictions regarding the effects of temperature on particles ejected from low index metal single crystals are presented.

II. SIMULATION

The general molecular dynamics scheme has been described in detail elsewhere.[18–22] Briefly the classical equations of motion are integrated in time using an interaction potential that describes the system of interest. The final velocities are used to calculate kinetic energy and angular distributions. The time evolution of the atomic motions is used to extract the important collision events.

The model system used approximates the Au{111} surface with a microcrystallite of 2016 atoms arranged in 9 layers of 224 atoms each. This crystal size is chosen such that the angular distributions are the same as those obtained for a selected set of impacts with a larger, more computationally intensive, crystal. These angular distributions were derived by integrating a series of calculated trajectories designed to mimic experimental data. These are an average over many individual collision cascades initiated by independent projectile impacts on the surface. Because the surface has translational and rotational symmetry, the array of impact points has been reduced to a triangular impact zone near the center of the crystal wherein each individual impact point is randomly chosen. The projectile is a 3 keV Ne atom. Open boundary conditions, rather than closed or periodic boundary conditions, are used so that particles are allowed to leave the sides and bottom of the crystal. This is essential to avoid the unrealistic confinement of atomic motions near the impact

point. The trajectories are terminated when the most energetic particle remaining in the solid has insufficient energy to overcome its attractive interactions. Finally, we verified that the shape of the angular distributions resulting from 10 keV Ne bombardment of Au{111} is essentially the same as obtained for 3 keV irradiation. The 3 keV system is chosen for the mechanistic analysis because a smaller crystal is sufficient to contain the collision cascade, hence the calculations are significantly less computationally intensive than for the larger crystal necessary for the 10 keV system.

Low and high temperature systems (0 and 550 K, respectively) were prepared by initially placing all atoms in the lattice in their bulk equilibrium configurations. This lattice was then relaxed to a local minimum whereby all particles have a velocity of zero. This point was assumed to correspond to 0 K. To obtain the high temperature lattice a generalized Langevin algorithm[23] was used to raise and equilibrate the average kinetic energy of the system to a value corresponding to 550 K. Two dimensional periodic boundary conditions were used during the equilibration process.[24] The system remained equilibrated for at least 100 picoseconds, much longer than the time required to evaluate a single collision cascade, with fluctuations of less than ± 5 K.

To describe the forces between the atoms, we employed an interaction potential constructed using the MD/MC-CEM approach.[25,26] The interaction energy, ΔE, of the entire system in MD/MC-CEM potentials is written as

$$\Delta E = \sum \Delta F_J(A_i;n_i) + \frac{1}{2}\sum_i \sum_j V_c(A_i,A_j),$$

where the set of atoms is $\{A_i,\ i=1,N\}$. The jellium density, n_i, is

$$n_i = \frac{1}{2}\sum_{j\neq i}^{N} \int \frac{n(A_i;\mathbf{r}-\mathbf{R}_i)}{Z_i}\, n(A_j;\mathbf{r}-\mathbf{R}_j)\,d\mathbf{r},$$

where $n(A_i;\mathbf{r}-\mathbf{R}_i)$ is the atomic electron density distribution as taken from Hartree-Fock calculations[27,28] and represented in even-tempered Gaussians[29] for computational ease. Z_i and R_i are the atomic number and nuclear position of the ith nuclei. The term ΔF_J is an empirical embedding function designated to ensure that the expression describes the properties of the atom in bulk and diatomic environments.[30] The embedding function is a characteristic of a particular atom type and is assumed not to depend on the source of the electron density. Thus, once this function is determined it can be used for any arbitrary configuration of atoms. The last term V_c is the Coulombic interaction between atoms A_i and A_j and is calculated from first principles. The MD/MC-CEM potential has recently been used in MD simulations of the keV particle bombardment of Ni{001} and Rh{001}.[17] The calculated energy resolved polar angle distributions for these crystal surfaces compare favorably with the experimentally obtained distributions. A Moliére potential was used to describe Ne-Au interactions.[31]

In order to establish computational convergence, we performed 1500 trajectories at 0 K and 3300 trajectories at 550 K. For the simulations at 0 K subsets of 110 trajectories were randomly selected from the larger set and the results were confirmed to preserve the primary angular features of interest. This selection of a smaller set is necessary because determination of atom ejection mechanisms is performed by visual inspection and is consequently time intensive.

The sampling procedure used to obtain the spectra of interest at 550 K is more complex. At elevated temperatures the mean vibrational displacement of the atoms in the lattice is not negligible, and several configurations of the lattice must be sampled. In order to insure that our sampling procedure is sufficient we evaluated results using two different methods. The first involves calculation of 110 trajectories on crystal lattices corresponding to the different crystal conformations at 22 evenly spaced time increments within a characteristic period of vibrational oscillation ($\sim$600 femtoseconds) of the central atom of the microcrystallite. A set of 110 trajectories corresponding to 5 random impact points at each of the 22 time steps is also generated to use in subsequent mechanistic analysis. Spectra obtained from the 110 trajectory subset preserve all the features of the larger set and the observables are not significantly affected by either the number of trajectories or the number of time steps used to sample at higher temperature. The smaller subset was used for mechanistic studies whereas the large set was used to obtain more statistically accurate angular distributions. To insure proper sampling of this dynamic substrate a second procedure was implemented in which the sampling of various crystal conformations occurs at 22 points in time chosen randomly. Each point is within a 500 femtosecond interval that occurs between 0 and 11 picoseconds. As in the first case, both the large and small set were generated at each of the 22 temporal sampling points. Each of these two sampling procedures yield very similar results. Based on this similarity, the mechanistic results presented are determined from the smaller 110 trajectory subset obtained using the former procedure.

The essence of the mechanistic evaluation method developed by Sanders *et al.*[16] is that the motion and energy of each ejected atom in the 110 trajectory set for each temperature can be extracted. This method is based on a technique developed by Harrison,[32] which he termed ''lean-on,'' a colloquial expression for a collision. The key point of the method is, therefore, the definition of a collision. We use a repulsive Moliére potential to define this event. At each integration step we check to see if the Moliére interaction between a pair of atoms is greater than a threshold energy. In this case a threshold value of 3 eV was chosen which allows the lean-on tree to be saved for at least 90% of the ejected atoms. If this value is obtained, then the event is flagged as a collision and new atoms are added to the lean-on tree. For each trajectory in the simulation a lean-on tree is determined. It is possible to scan through the saved lean-on information and extract the positions and velocities of the ''trace atoms'' involved in the momentum transfer sequence which eventually ejects the atom of interest. By graphically evaluating the processes of momentum transfer the reoccurring sequences of events can be mechanistically categorized and, hence the change in specific angular features as a function of sample temperature can be understood from the microscopic perspective.

The experimental data of Szymczak and Wittmaack were collected with an angular resolution of approximately 3°. Our angular spectra are collected with an angular resolution

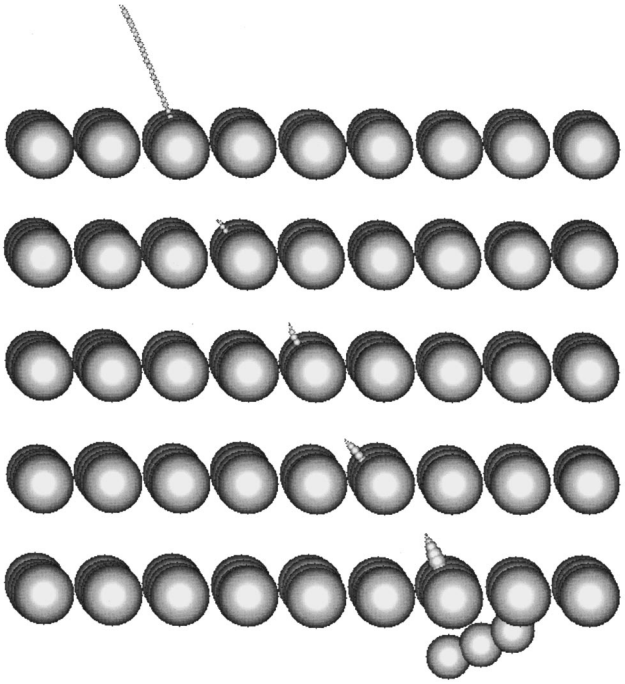

FIG. 2. Time lapse representation of a trajectory which leads to ejection of an atom into the [110] spot. The size of the moving atoms reflects their instantaneous total (kinetic+potential) energy and their positions are plotted at 5-fs intervals. The diameter of the rigid crystal atoms is equivalent to a 40-eV total energy. The view is from the [010] direction.

of 6°. This value is chosen because it is small enough to not significantly alter the features of interest, yet large enough to give a high signal to noise ratio and smooth spectra.

III. RESULTS AND DISCUSSION

Shown in the bottom section of Fig. 1 is the energy integrated polar-angle spectra of ejected atoms obtained from the MD calculations. The experimental spectra of Szymczak and Wittmaack[7] are displayed in the top frame of Fig. 1. The two sets of results are qualitatively similar. The simulation reproduces the change in yield along the [110] direction and the [100] direction as a function of temperature. The ratio of the peak heights for the [110] spot at low and high temperatures is found to be 2.2 ± 0.1 using the 6° angular resolution detector. If we calculate these spectra with the experimental angular resolution of 3° the ratio of the yields is 3.1 ± 0.3.[33] This is in excellent agreement with the experimentally obtained ratio of 3.5 as determined by Szymczak and Wittmaack. It is also observed that emission along the [100] direction decreases with increased temperature although uncertainty in both the calculated and experimental distributions does not allow performing a more quantitative analysis. Finally, the overall angle-integrated ejection yield from our calculation decreases by only about 20% between 0 and 550 K.

We now focus on the microscopic processes which are responsible for the observed temperature effects. Shown in Fig. 2 is a pictorial representation of the events preceding one ejection process which is used to trace the path of momentum transfer after ion impact and to categorize the events which lead to ejection. Each plot has two parts, the first

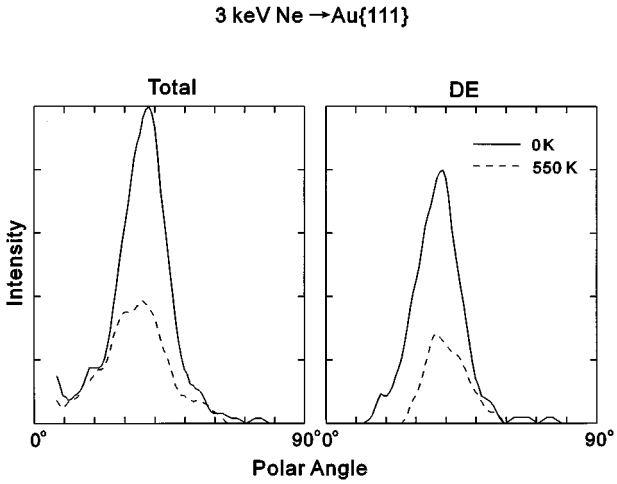

FIG. 3. Shown on the left is the energy integrated polar angle distribution in the $\varphi=-30°$ azimuthal direction for all atoms which ejected as the result of 3 keV Ne atom bombardment. On the right are the distributions for only the DE sequence ejection channel. These spectra are calculated from the 110 trajectory set.

being the lattice atoms in their initial positions (prior to bombardment) and the second being the positions of the several trace atoms shown at 5-fs intervals. The radius of the trace atoms is proportional to their instantaneous total (kinetic +potential) energy. The fixed crystal atoms are drawn with a radius which is equivalent to 40 eV of total energy. This graphical representation depicts the time dependence of the positions and energy of the trace atoms in a compact form. Moreover, the motions of the remainder of the atoms are not shown and thus do not visually detract from the motions of the particles of interest. The advantage of this graphical representation is that the picture is sufficiently simple that virtually all the ejection events can be viewed in order to obtain a perspective of the important collisions. Note, however, that the pictures suggest that only a few atoms are moving during the ejection sequence. It is important to remember that many atoms do move from their original positions.

The sequence in Fig. 2 is extracted from our calculations. For this trajectory, the Ne projectile has deposited a portion of its momentum several layers beneath the surface. This initially deposited momentum eventually is transferred back to the surface in a directional collision sequence as shown. This particular ejection sequence extends over four nearest neighbor units along a close packed crystallographic direction and the surface atom ejects into the [110] spot. Processes such as these are loosely termed focusons in the nomenclature initially set forth by Silsbee.[34] It is important to note that our analysis also includes events of unit length (i.e., nearest-neighbor collisions) which usually are not categorized in the Silsbee model. Therefore, we prefer to be more grammatically explicit and denote all sequences propagating along close-packed crystallographic directions as direct ejection (DE) sequences. Szymczak and Wittmaack proposed that the temperature effects observed for Au{111} could be related to the change in contribution of this channel to the ejection yield with temperature. Our technique allows us to address the validity of this proposal via the mechanistic monitoring of the ejected atoms as a function of temperature.

Displayed in Fig. 3 are the mechanistically resolved an-

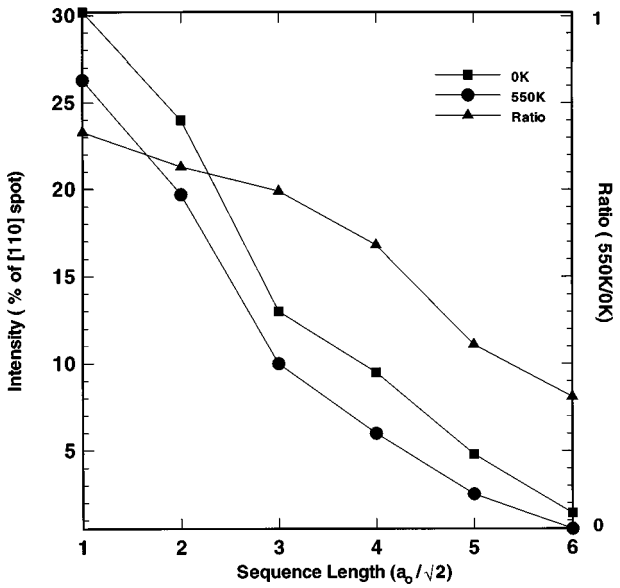

FIG. 4. Shown using the right axis and the solid triangles is the ratio of the number of particles ejected at 550 K to the number of particles ejected at 0 K versus the length of the direct ejection (DE) sequence. Displayed with solid squares and circles, using the left axis, is the relative contribution of DE sequences of various lengths to the total emission into the [110] spot. The nearest-neighbor spacing along the [110] direction is $a_0/\sqrt{2}$ where a_0 is the lattice constant.

gular distributions for the temperatures of interest. On the left are the polar-angle spectra along the [110] direction integrated over all atoms independent of ejection mechanism. Depicted in the right frame of Fig. 3 are the angular contributions for the set of particles which are ejected via the DE channel of desorption. At 0 K DE sequences are responsible for about eight in every ten ejections into the [110] spot and about one in every two ejections regardless of the polar and azimuthal angles of ejection. This value is much higher than for other less densely packed crystal faces. For instance the {001} surface has been shown to have a contribution of less than 10% from direct ejection sequences to the overall yield.[17] We find that 90%±5% of the temperature related change in the ejection yield in the [110] spot is the result of depletion in this channel.

In an effort to quantify the temperature effect, the number of DE sequences present in the [110] spot as a function of the length of the sequence have been determined from the simulations at both temperatures and are shown in Fig. 4. Also shown is the ratio of the number of DE events at 550 to 0 K versus sequence length. At both temperatures the DE sequences of shorter length contribute more to the [110] spot than do the longer sequences. In addition, the ratio decreases with increasing temperature. The latter observation agrees with the temperature dependent scenario proposed by Szymczak and Wittmaack in which the observed decrease of the yield in the [110] spot is related to a subsurface misalignment of long-range replacement sequences. In concurrence with our proposal, the long sequences are more affected by temperature than the short ones. On the other hand, as also displayed in Fig. 4, the shorter events are responsible for the major contribution to the yield in the [110] spot and account for the majority of the observed temperature effect. In particular, the observed temperature dependence of DE sequences of unit length is solely attributed to the surface. These observations clearly reinforce the point of view that the relative positions of the atoms in the near surface region dictate the evolution of the ejection event.[2,11]

Using angle-resolved secondary ion mass spectrometry, Lauderback *et al.* have measured the azimuthal angular distributions of Ni^+ ions ejected from the Ni{111} surface with energies of 10 eV ±3 eV and within the polar angle range of 45±7.5 as a function of sample temperature.[7] A decrease in the ratio of the maximum peak intensity along the $\varphi=30°$ to $\varphi=0°$ directions was observed as the sample temperature was increased. This effect is also evident in our simulations, although not as prominently as when the temperature dependence of ejection along the $\varphi=-30°$ direction is considered. This deviation can be associated with the fact that Lauderback *et al.* evaluated a specific subset of ejection energy and polar angles, whereas our simulations are energy integrated for all polar angles. In fact, if we limit our analysis to a specific subset of ejection energy and polar angles we find the temperature dependence along the $\varphi=30°$ azimuth becomes increasingly important.

Our calculations indicate that the magnitude of the temperature effect on the angular spectra decreases as the energy of emitted particles increases. This observation suggests one reason why previous calculations, which did not incorporate sample temperature, were better able to reproduce the high energy part of the experimental angular spectra then the spectra for particles emitted with low kinetic energies.[11–14,21]

Another topic of interest is the ability to predict the relative temperature effect on low index crystal faces. As discussed previously, we believe that the observed temperature effect is caused predominantly by vibrationally induced alteration of the innate surface registry with some minor contribution of subsurface misalignment of long chain DE sequences. This implies that the activity of the observed temperature-dependent changes in yield should be strongly dependent on the packing density of a given surface. To address these issues we have plotted in Fig. 5 the contribution of DE sequences to the total yield for simulations at 0 K and also for our previous simulations on Ni{001} and Rh{001}.[17] As with the {111} surface, the most intense feature in the angular distribution for the {001} surface is a [110] spot. The relative contribution of the DE channel is larger for the {111} surface than for the less densely packed {001} crystal face, especially for sequences of 1 and 2 nearest-neighbor units. Based on these observations we propose that the temperature effect on a given single crystal metal surface will be such that the more densely packed and higher vibrationally active substrates should demonstrate the largest temperature effect. Considering these factors we expect that for ion bombarded fcc metals the order of decreasing temperature effect for various low index crystal faces will be such that {111}>{100}>{110}. This proposal is supported by experiments on Ni{001} in which we observe no change in the polar-angle spectra as a function of varying target temperature.[35] As emphasized in this work the observed temperature effect is largest along ejection directions which are close-packed crystallographic directions, namely the [110] directions for fcc metals, although desorption along the other azimuths is also affected. An interesting system to address using our predic-

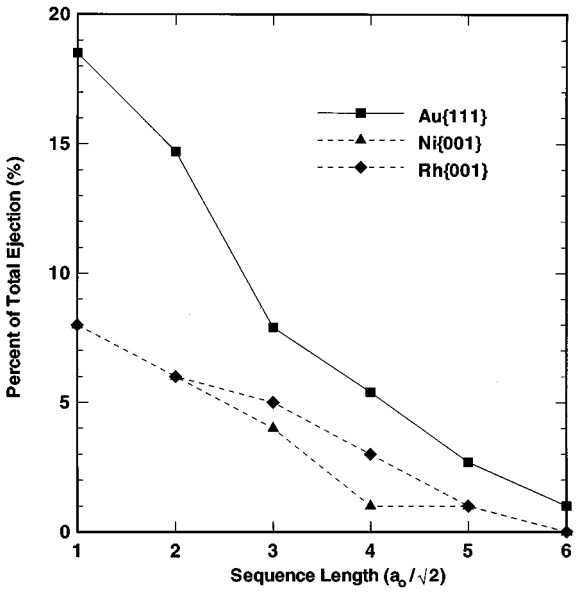

FIG. 5. Shown is the percent of overall ejection versus the chain length of direct ejection sequences for both {111} and {001} fcc metal surfaces investigated at classical 0 K temperature.

tions of temperature activity is the fcc {331} surface on which two of the [110] directions ($\phi=-30°$, 210°) are initially blocked because of the innate registry of the lattice while the third close-packed direction ($\phi=90°$) is not initially blocked. In this system we would expect the [110] spot along $\phi=90°$ to be most affected by temperature.

IV. CONCLUSIONS

The polar-angle spectra for keV ion bombarded Au{111} have been calculated for different target temperatures using molecular dynamics simulations. The results are found to be remarkably similar to those obtained experimentally by Szymczak and Wittmaack. We have used graphical analysis software to evaluate the mechanism responsible for the observed effects of temperature on the polar-angle distributions of Au{111}. Based on this analysis we find that about 90% of the decrease in the yield of the [110] spot between 0 and 550 K is affiliated with a decrease in the contribution of DE sequences along close packed crystallographic directions of the lattice. We find that the observed temperature-dependent decrease in yield along the [110] ejection direction results from predominately surface quenching with some minor contribution from subsurface misalignment of direct ejection sequence chains. The contribution of DE sequences clearly depends on the crystal face of interest. We predict that the observed temperature dependence should be most apparent for densely packed, vibrationally active surfaces. This study contributes to the relatively small published database on the effects of temperature on the ejection process and can be used to predict the effect of temperature on other crystal faces as well as assisting in the deconvolution of the massively complex ejection process.

ACKNOWLEDGMENTS

The authors wish to thank J. S. Burnham, D. E. Sanders, R. Chatterjee, D. E. Riederer, E. J. Dawnkaski, W. Szymczak, and K. Wittmaack for fruitful discussions. The financial support of the U.S. Office of Naval Research, U.S. National Science Foundation, the SUR Program of the IBM Corporation, and the M. Curie-Sklodowska fund No. MEN/NSF-93-144 is gratefully acknowledged.

[1] G. K. Wehner, J. Appl. Phys. **26**, 1056 (1955).
[2] N. Winograd, Mat. Fys. Dan. Vid. Selsk. **43**, 223 (1993).
[3] The specific temperature effect addressed in this manuscript is the result of increased vibrational amplitudes as opposed to the scenario of temperature dependent effects which are the result of passing through a phase transition and changing the equilibrium registry for a given set of experimental conditions.
[4] M. T. Robinson, in *Sputtering by Particle Bombardment*, edited by R. Behrisch (Springer-Verlag, Berlin, 1981), p. 73 and references cited therein.
[5] C. Lehman and P. Sigmund, Phys. Status Solidi **16**, 507 (1966).
[6] P. Sigmund, Phys. Rev. **184**, 383 (1969); **187**, 768 (1969).
[7] W. Szymczak and K. Wittmaack, Nucl. Instrum. Methods B **82**, 220 (1993).
[8] L. L. Lauderback, Y. Zhang, and R. Nge, Phys. Rev. B **48**, 1750 (1993).
[9] In previous investigations of {111} crystal faces we refer to the [110] peak as the off-normal peak along the $-30°$ azimuth.
[10] In previous investigations of {111} crystal faces we refer to the [100] peak as the off-normal peak along the $+30°$ azimuth.
[11] N. Winograd, B. J. Garrison, and D. E. Harrison, Jr., Phys. Rev. Lett. **41**, 1120 (1978).
[12] N. Winograd, P. H. Kobrin, G. A. Schick, J. Singh, J. P. Baxter, and B. J. Garrison, Surf. Sci. **176**, L817 (1986).
[13] B. J. Garrison, C. T. Riemann, N. Winograd, and D. E. Harrison, Phys. Rev. B **36**, 3516 (1987).
[14] R. Maboudian, Z. Postawa, M. El-Maazawi, B. J. Garrison, and N. Winograd, Phys. Rev. B **42**, 7311 (1990).
[15] N. Winograd, B. J. Garrison, and D. E. Harrison, Jr., Phys. Rev. Lett. **41**, 1120 (1978).
[16] D. E. Sanders, K. B. S. Prasad, J. S. Burnham, and B. J. Garrison, Phys. Rev. B **50**, 5358 (1994).
[17] S. W. Rosencrance, J. S. Burnham, D. E. Sanders, C. He, B. J. Garrison, N. Winograd, Z. Postawa, and A. E. DePristo, Phys. Rev. B **52**, 6006 (1995).
[18] D. E. Harrison, Jr., CRC Crit. Rev. Solid State Mater. Sci. **14**, 51 (1988).
[19] B. J. Garrison, Chem. Soc. Rev. **21**, 155 (1992).
[20] B. J. Garrison, N. Winograd, and D. E. Harrison, Jr., J. Chem. Phys. **69**, 1440 (1978).
[21] B. J. Garrison, N. Winograd, D. M. Deaven, C. T. Reimann, D. Y. Lo, T. A. Tombrello, and M. H. Shapiro, Phys. Rev. B **37**, 7197 (1988).
[22] D. N. Bernardo, R. Bhatia, and B. J. Garrison, Comput. Phys. Commun. **80**, 259 (1994).

[23] R. R. Lucchese and J. C. Tully, Surf. Sci. **137**, 570 (1983).
[24] D. Y. Lo, M. H. Shapiro, T. A. Tombrello, B. J. Garrison, and N. Winograd, in *Beam-Solid Interactions and Transient Processes*, edited by M. O. Thompson, S. T. Picraux, and J. S. Williams, MRS Symposia Proceedings No. 74 (Materials Research Society, Pittsburgh, 1987), p. 449.
[25] M. S. Stave, D. E. Sanders, T. J. Raeker, and A. E. DePristo, J. Chem. Phys. **93**, 4413 (1990).
[26] T. J. Raeker and A. E. DePristo, Int. Rev. Phys. Chem. **10**, 1 (1991).
[27] E. Clementi, IBM J. Res. Dev. Suppl. **9** (1965).
[28] P. S. Bagus, T. L. Gilbert, and C. J. Roothan, J. Chem. Phys. **56**, 5159 (1972).
[29] M. Schmidt and K. Ruedenberg, J. Chem. Phys. **71**, 3951 (1979).
[30] C. L. Kelchner, D. M. Halstead, L. S. Perkins, N. M. Wallace, and A. E. DePristo, Surf. Sci. **310**, 425 (1994).
[31] The unscaled Firsov screening length was used. The complete Moliére equation is given in D. J. O'Connor and R. J. MacDonald, Radiat. Eff. **34**, 247 (1977).
[32] This terminology dates back to at least 1977, when we inherited the computer code from D. E. Harrison, Jr.
[33] The dependence of the ratio of the peak heights at different temperatures on the angular resolution of the detector is because the [110] spot shape depends on temperature. This has also been previously observed by Szymczak and Wittmaack.
[34] R. H. Silsbee, J. Appl. Phys. **28**, 1246 (1957).
[35] Z. Postawa, C. He, S. W. Rosencrance, R. Chatterjee, and N. Winograd (unpublished).